

Rapid emplacement of massive Duluth Complex intrusions within the Midcontinent Rift

Nicholas L. Swanson-Hysell¹, Steven A. Hoaglund², James L. Crowley³, Mark D. Schmitz³, Yiming Zhang¹, James D. Miller Jr.²

¹ Department of Earth and Planetary Science, University of California, Berkeley, CA, USA

² Department of Earth and Environmental Sciences, University of Minnesota, Duluth, MN, USA

³ Department of Geosciences, Boise State University, Boise, ID, USA

ABSTRACT

The Duluth Complex is one of the largest mafic intrusive complexes on Earth. It was emplaced as the Midcontinent Rift developed in Laurentia's interior during an interval of magmatism and extension from *ca.* 1109 to 1084 Ma. This duration of magmatic activity is more protracted than is typical for large igneous provinces interpreted to have formed from decompression melting of upwelling mantle plumes. While the overall duration was protracted, there were intervals of more voluminous magmatism. New $^{206}\text{Pb}/^{238}\text{U}$ zircon dates for the anorthositic and layered series of the Duluth Complex constrain these units to have been emplaced *ca.* 1096 Ma in less than one million years (duration of $500,000 \pm 260,000$ years). Comparison of paleomagnetic data from these units with Laurentia's apparent polar wander path supports this interpretation. This rapid emplacement bears similarities to the geologically short duration of well-dated large igneous provinces. These data support hypotheses that call upon the co-location of lithospheric extension and anomalously hot upwelling mantle. This rapid magmatic pulse occurred more than 10 million years after initial magmatism following more than 20° of latitudinal plate motion. A likely scenario is one in which upwelling mantle encountered the base of Laurentian lithosphere and flowed via "upside-down drainage" to locally thinned lithosphere of the Midcontinent Rift.

¹⁷ INTRODUCTION

¹⁸ The Midcontinent Rift represents a protracted tectonomagmatic event in the interior of Laurentia
¹⁹ (the North American craton). Voluminous outpouring of lava and emplacement of intrusions
²⁰ accompanied rift development (Fig. 1). Magmatic activity initiated *ca.* 1109 Ma and continued
²¹ until *ca.* 1084 Ma (Swanson-Hysell et al., 2019). Preserved thicknesses of the volcanic successions
²² range from nearly 10 km for partial sections exposed on land, (Green et al., 2011), to ~25 km
²³ under Lake Superior (Cannon, 1992). These volcanics and associated intrusions are much more
²⁴ voluminous than is typical for tectonic rifting. Analysis of seismic data leads to an estimate that
²⁵ total eruptive volume exceeded 2×10^6 km³ with a greater volume added to the lithosphere as
²⁶ intrusions and a magmatic underplate (Cannon, 1992). The ~25 Myr duration of Midcontinent
²⁷ Rift volcanism is much longer than is typical for large igneous province emplacement associated
²⁸ with decompression melting of an upwelling mantle plume. Well-dated large igneous provinces,
²⁹ such as the Central Atlantic Magmatic Province (Blackburn et al., 2013), the Karoo-Ferrar
³⁰ (Burgess et al., 2015), and the Deccan Traps (Schoene et al., 2019; Sprain et al., 2019) have
³¹ durations of <1 Myr for the bulk of their magmatism. An explanation for prolonged volcanism in
³² the Midcontinent Rift could attribute rift initiation and initial volcanism via plume arrival with
³³ continued volcanism resulting from rift-driven asthenospheric upwelling. However, the most
³⁴ voluminous period of magmatism occurred more than 10 million years after initial flood volcanism
³⁵ during an interval known as the “main magmatic stage” (Vervoort et al., 2007). Main stage
³⁶ magmatism has been attributed to an upwelling mantle plume based on the large volume and
³⁷ geochemical signatures (Nicholson and Shirey, 1990; White and McKenzie, 1995).

³⁸ Pioneering Midcontinent Rift geochronology utilized $^{207}\text{Pb}/^{206}\text{Pb}$ dates on zircon from
³⁹ volcanics (Davis and Green, 1997) and intrusions (Paces and Miller, 1993) to illuminate the
⁴⁰ magmatic history. Subsequent advances in U-Pb geochronology enable higher precision
⁴¹ $^{206}\text{Pb}/^{238}\text{U}$ dates to be used when chemical abrasion methods have mitigated Pb loss (Mattinson,
⁴² 2005). U-Pb dates developed using these methods have led to an updated chronostratigraphic

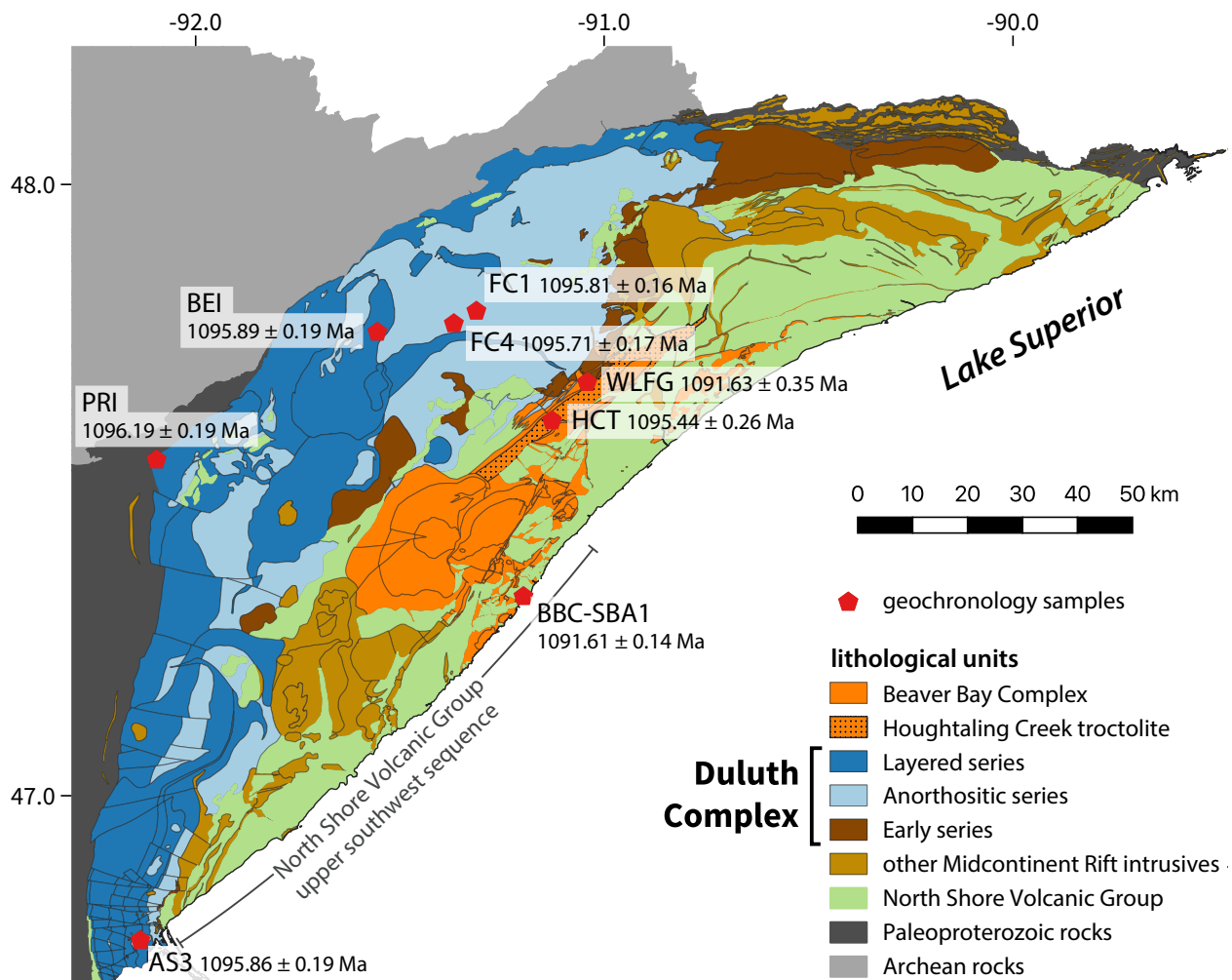


Figure 1. Geologic map of NE Minnesota (simplified from Jirsa et al., 2011) highlighting Midcontinent Rift intrusive complexes and geochronology sample locations. Volcanic and intrusive units dip towards Lake Superior typically at 10° to 20° . U-Pb dates from the anorthositic and layered series of the Duluth Complex (light and dark blue) indicate rapid emplacement in less than 1 million years.

43 framework for Midcontinent Rift volcanics (Swanson-Hysell et al., 2019; Fig. 2). With these
 44 higher precision constraints, the timing and tempo of magmatic activity within the rift can be
 45 reevaluated – was it continuous or punctuated by pulses? Key to evaluating this question is the
 46 timing of emplacement of intrusive rocks, particularly the largest intrusive suite – the Duluth
 47 Complex (Fig. 1). With its arcuate area of 5630 km^2 , the tholeiitic Duluth Complex is the
 48 second-largest exposed mafic intrusive complex on Earth (Miller et al., 2002). It was emplaced as
 49 sheet-like intrusions into the base of a comagmatic volcanic succession with the majority of its

50 volume associated with the anorthositic series and the layered series of gabbroic and troctolitic
51 cumulates (Miller et al., 2002; Fig. 1). We present $^{206}\text{Pb}/^{238}\text{U}$ zircon dates from the Duluth
52 Complex, as well as the Beaver Bay Complex, to improve constraints on the duration of intrusive
53 magmatism and contextualize it with the chronology of volcanism.

54 METHODS and RESULTS

55 Zircon crystals were chemically abraded prior to analysis by isotope dilution thermal ionization
56 mass spectrometry (ID-TIMS).¹ Weighted means were calculated from multiple single zircon
57 dates (Fig. 2 and Table 1). These $^{206}\text{Pb}/^{238}\text{U}$ dates can be compared to one another, and to the
58 volcanic dates of Swanson-Hysell et al. (2019), at the level of analytical uncertainty (X uncertainty
59 in Table 1) given that all dates were developed using EARTHTIME tracer solutions (Condon
60 et al., 2015). This 2σ analytical uncertainty will be reported when dates are discussed. External
61 uncertainties and mean squared weighted deviation (MSWD) values are reported in Table 1.

62 The Duluth Complex anorthositic series comprises plagioclase-rich gabbroic cumulates varying
63 from anorthositic gabbro to anorthosite. Samples FC1 and FC4b are from gabbroic anorthosite
64 exposures near the former logging town of Forest Center. A weighted mean $^{206}\text{Pb}/^{238}\text{U}$ date for
65 FC1 of 1095.81 ± 0.16 Ma is calculated based on 10 single zircon dates (Table 1). This date is
66 indistinguishable from a weighted mean $^{206}\text{Pb}/^{238}\text{U}$ date for FC1 of 1095.97 ± 0.22 Ma developed
67 by Ibañez-Mejia and Tissot (2019). Our new FC4b date is indistinguishable from these FC1 dates
68 with a weighted mean $^{206}\text{Pb}/^{238}\text{U}$ date of 1095.69 ± 0.18 Ma based on dates from 7 zircons.
69 These dates are indistinguishable from the weighted mean $^{206}\text{Pb}/^{238}\text{U}$ date of 1095.86 ± 0.19 Ma
70 developed from chemically-abraded zircons of anorthositic series sample AS3 collected in Duluth
71 (Schoene et al., 2006; Fig. 2, Table 1). Zircon grains from these anorthositic series samples are

¹GSA Data Repository item 2020XXX, individual zircon dates, paleomagnetic site mean directions, and additional method details are available online at <http://www.geosociety.org/datarerepository>. Paleomagnetic data and interpreted directions are in the MagIC database (<https://earthref.org/MagIC/doi/ADDINPROOFS>). Geochronological data are available at <https://www.Geochron.org>. Code associated with statistical tests and data visualization is available in a Zenodo repository <https://zenodo.org/record/ADDINPROOFS>.

72 commonly used as U-Pb standards.

73 The layered series of the Duluth Complex is a suite of stratiform troctolitic to gabbroic
 74 cumulates emplaced as discrete intrusions (Fig. 1). The PRI sample is an augite troctolite from
 75 the Partridge River intrusion which is at the base of the complex in contact with underlying
 76 Paleoproterozoic metasedimentary rocks (Fig. 1). Data from 6 zircons result in a weighted mean
 77 $^{206}\text{Pb}/^{238}\text{U}$ date of 1096.19 ± 0.19 Ma (Fig. 2). The BEI sample is an olivine gabbro from the
 78 Bald Eagle intrusion. This intrusion has been interpreted as one of the youngest layered series
 79 units based on cross-cutting relationships inferred from aeromagnetic data (Miller et al., 2002).
 80 Dates from 6 zircons of BEI result in a weighted mean $^{206}\text{Pb}/^{238}\text{U}$ date of 1095.89 ± 0.19 Ma
 81 (Fig. 2).

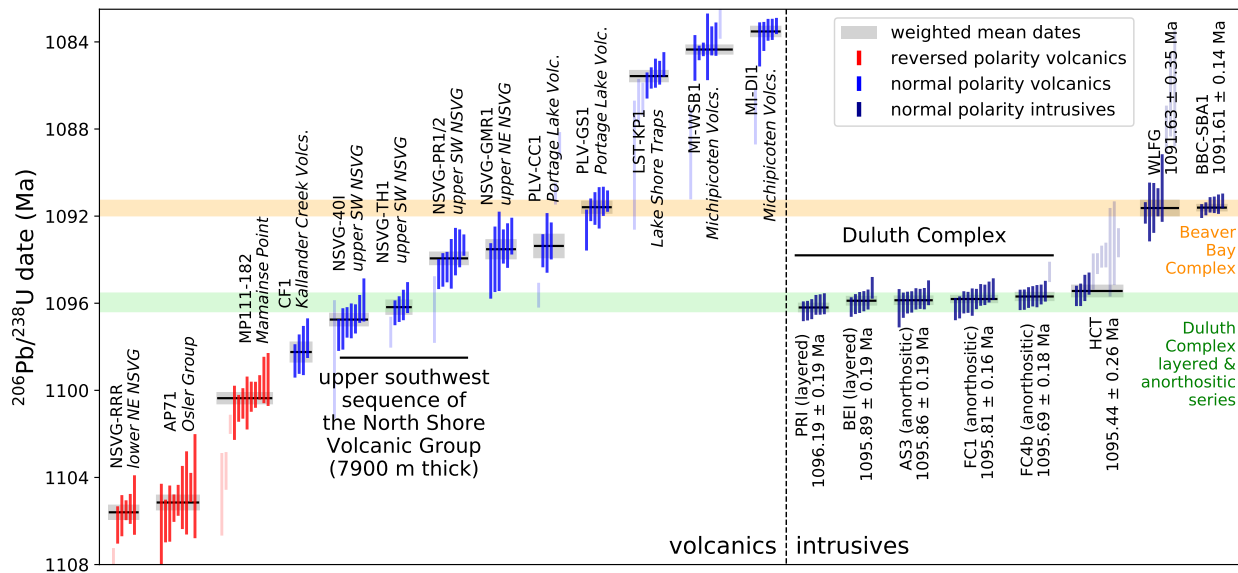


Figure 2. Date bar plot of CA-ID-TIMS $^{206}\text{Pb}/^{238}\text{U}$ zircon dates for Midcontinent Rift volcanics and intrusives. Dates for volcanics and BBC-SBA1 are from Fairchild et al. (2017) and Swanson-Hysell et al. (2019). The AS3 date is from Schoene et al. (2006). Each vertical bar represents the date for an individual zircon while the horizontal lines and grey boxes represent the weighted means and their uncertainty.

82 The Beaver Bay complex is a suite of dominantly hypabyssal intrusions that cross-cut the
 83 North Shore Volcanic Group (Fig. 1). Sample HCT is an augite troctolite from the Houghtaling
 84 Creek troctolite macrodike (Miller et al., 2001). In contrast to the internally-consistent dates
 85 from the layered and anorthositic series samples, $^{206}\text{Pb}/^{238}\text{U}$ zircon dates from HCT have more

dispersion that we interpret as resulting from Pb loss not fully mitigated by chemical abrasion. After excluding individual dates that trend away from concordia, dates from 4 concordant zircons result in a weighted mean $^{206}\text{Pb}/^{238}\text{U}$ date of 1095.44 ± 0.26 Ma (Fig. 2). A sample of ferrodiorite was collected as WLFG from the Wilson Lake ferrogabbro of the Beaver Bay Complex. This plug-shaped zoned intrusion was emplaced into the Duluth Complex roof zone. Variable intensity chemical abrasion was applied to WLFG zircons with hotter and longer dissolution yielding more concordant data with older $^{206}\text{Pb}/^{238}\text{U}$ dates (Table DR1). After excluding those interpreted to have unmitigated Pb loss, dates from 5 zircons result in a weighted mean $^{206}\text{Pb}/^{238}\text{U}$ date of 1091.63 ± 0.35 Ma (Fig. 2). This date is indistinguishable from the 1091.61 ± 0.14 Ma $^{206}\text{Pb}/^{238}\text{U}$ date of a Silver Bay intrusion within the Beaver Bay Complex (BBC-SBA1 of Fairchild et al., 2017; Figs. 1 and 2).

Table 1. Summary of CA-ID-TIMS $^{206}\text{Pb}/^{238}\text{U}$ dates from Midcontinent Rift intrusions

Sample	Group	Latitude Longitude	$^{206}\text{Pb}/^{238}\text{U}$ date (Ma)	Uncertainty (2σ) X Y Z	MSWD	n/N
PRI <i>Partridge River Intrusion</i> augite troctolite	Duluth Complex (layered series)	47.5480° N 92.1074° W	1096.19	0.19 0.36 1.15	0.45	6/6
BEI <i>Bald Eagle Intrusion</i> olivine gabbro	Duluth Complex (layered series)	47.7516° N 91.5680° W	1095.89	0.19 0.36 1.15	1.59	6/6
AS3 <i>Duluth gabbroic anorthosite</i>	Duluth Complex (anorthositic series)	46.7621° N 92.1590° W	1095.86	0.19 0.36 1.15	0.43	8/8
FC1 <i>Forest Center gabbroic anorthosite</i>	Duluth Complex (anorthositic series)	47.7827° N 91.3266° W	1095.81	0.16 0.34 1.14	1.44	10/10
FC4b <i>Forest Center gabbroic anorthosite</i>	Duluth Complex (anorthositic series)	47.7677° N 91.3753° W	1095.69	0.18 0.35 1.14	0.34	7/8
HCT <i>Houghtaling Creek Troctolite</i>	Beaver Bay Complex	47.6009° N 91.1497° W	1095.44	0.26 0.40 1.16	1.13	4/11
WLFG <i>Wilson Lake Ferrogabbro</i> ferrodiorite	Beaver Bay Complex	47.6620° N 91.0619° W	1091.63	0.35 0.46 1.18	0.74	5/8
BBC-SBA1 <i>Silver Bay aplite</i>	Beaver Bay Complex	47.6620° N 91.0619° W	1091.61	0.14 0.30 1.2	1.0	6/6

Notes: X is 2σ analytical uncertainty; Y is 2σ uncertainty also incorporating tracer calibration for comparison to U-Pb dates not developed using EARTHTIME-calibrated tracer solutions; Z is 2σ uncertainty including X and Y, as well as ^{238}U decay constant uncertainty (0.108%; Jaffey et al., 1971). This Z uncertainty needs to be utilized when comparing to dates using other decay systems (e.g., $^{40}\text{Ar}/^{39}\text{Ar}$, $^{187}\text{Re}-^{187}\text{Os}$); MSWD is the mean squared weighted deviation; n is the number of individual zircon dates included in the calculated sample mean date; N is the number of individual zircons analyzed for the sample. All dates are from this study with the exceptions of AS3 (Schoene et al., 2006) and BBC-SBA1 (Fairchild et al., 2017).

97 Paleomagnetic data from the layered series (37 sites) and the anorthositic series (11 sites) near
 98 Duluth were published in Beck (1970) (Fig. 3). Site directions of the layered and anorthositic
 99 series share a common mean, consistent with their overlapping U-Pb dates. In order to pair
 100 paleomagnetic data with geochronology, oriented cores were collected and analyzed from the sites
 101 of FC1, FC4 and HCT. Magnetization was measured on a 2G DC-SQUID magnetometer at
 102 Berkeley. Samples underwent alternating field (AF) or thermal demagnetization steps and fits
 103 were made using PmagPy (Tauxe et al., 2016). While Beck (1970) did not implement tilt
 104 corrections, the Duluth Complex and overlying lavas dip towards Lake Superior and
 105 paleomagnetic data need to be corrected for this tilt. We compile abundant igneous layering
 106 orientations, which are similar to the tilt of overlying lavas and interflow sediments, and use them
 107 for tilt correction.

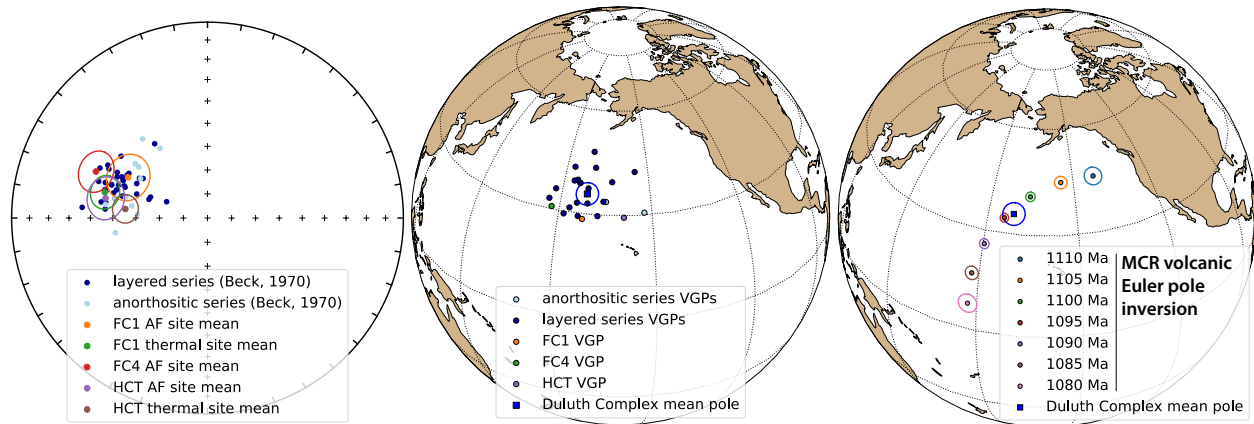


Figure 3. Left panel: tilt-corrected site mean paleomagnetic directions from anorthositic and layered series sites of Beck (1970) and from the FC1, FC4, and HCT sites. Center panel: Virtual geomagnetic poles (VGPs) for sites with $\alpha_{95} < 15^\circ$ give a mean pole of: 188.7° E, 35.6° N, $N=24$, $A_{95}=3.1$, $k=92$. Right panel: Duluth Complex pole shown with a synthesized pole path developed from Midcontinent Rift volcanic poles.

108 Rapid progression of poles within the apparent polar wander path (APWP) enable these
 109 paleomagnetic data to give chronological insight. Pole positions from the early stage of rift
 110 magmatism are different from main stage lavas (Fig. 3). The similar position of Duluth Complex
 111 layered and anorthositic series virtual geomagnetic poles (VGPs) is consistent with
 112 contemporaneous emplacement and they can be combined into a mean pole (Fig. 3). This pole

113 can be compared to a synthesized APWP developed using an Euler pole inversion of
114 chronostratigraphically-controlled volcanic poles (Swanson-Hysell et al., 2019). The Duluth
115 Complex pole lies between the 1100 Ma and 1095 Ma path positions with the A_{95} uncertainty of
116 the pole overlapping with the two angular standard deviations ellipse of the 1095 Ma path
117 position. This result is consistent with a *ca.* 1096 Ma age for the layered and anorthositic series
118 and strengthens the correlation with the volcanics.

119 **DISCUSSION**

120 The new U-Pb dates, together with paleomagnetic data, imply that the bulk of the Duluth
121 Complex layered series and anorthositic series were emplaced in less than 1 million years. The age
122 differences between the anorthositic series and BEI layered series dates are all within uncertainty
123 of no difference. The Partridge River intrusion layered series date is slightly older with an age
124 difference from the rest of the anorthositic and layered series dates that is distinct from zero at
125 95% confidence. Taking this oldest date of 1096.19 ± 0.19 Ma for PRI and the youngest date of
126 1095.69 ± 0.18 Ma from FC4b yields a duration of overall emplacement of the layered and
127 anorthositic series of $500,000 \pm 260,000$ years (2σ). This emplacement was coeval with eruption of
128 the North Shore Volcanic Group (NSVG) upper southwest sequence which comprises ~ 7900
129 meters of lavas and is the thickest exposed Midcontinent Rift volcanic succession (Fig. 1; Green
130 et al., 2011; Swanson-Hysell et al., 2019). This rapid emplacement of the bulk of the Duluth
131 Complex, together with coeval NSVG eruptions, require a large pulse of melt generation *ca.* 1096
132 Ma.

133 The 1095.44 ± 0.26 Ma age of the Houghtaling Creek troctolite is indistinguishable from the
134 youngest anorthositic series date. This result indicates that this pulse of voluminous magmatic
135 activity is represented in some Beaver Bay Complex intrusions. A younger pulse of Beaver Bay
136 Complex magmatism postdates NSVG eruptions as units such as the Silver Bay intrusions
137 penetrate the youngest NSVG lavas, including the 1093.94 ± 0.28 Ma Palisade Rhyolite (Miller

et al., 2001; Swanson-Hysell et al., 2019; Fig. 1). The age of this magmatism is constrained by indistinguishable dates of 1091.63 ± 0.35 Ma for the Wilson Lake ferrogabbro and 1091.61 ± 0.14 Ma from the Silver Bay intrusions (Fig. 2; Table 1). This younger Beaver Bay Complex magmatism is coeval with eruption of the >5 km thick Portage Lake Volcanics that are exposed on the Keweenaw Peninsula and Isle Royale (Fig. 2).

Rapid emplacement of the voluminous layered and anorthositic series of the Duluth Complex bears similarities to the geologically short duration (<1 Myr) of well-dated flood basalt provinces (Burgess et al., 2015; Schoene et al., 2019). This similarity supports the hypothesis put forward by Green (1983), and advanced by others including Cannon and Hinze (1992) and Stein et al. (2015), that co-location of massive magmatism and rifting is the result of lithospheric extension atop decompression melting of an upwelling mantle plume. Contemporaneous heating of Laurentia lithosphere 600 km to the north of the rift is indicated by thermochronologic data from middle to lower crustal xenoliths (Edwards and Blackburn, 2018). Basaltic magma was also emplaced throughout the Southwest large igneous province coeval with rift magmatism, including sills more than 2300 km from Duluth (Bright et al., 2014). That such a broad region of Laurentia lithosphere experienced heating and magmatism supports hypothesized large-scale mantle upwelling.

Both the *ca.* 1108 early stage and *ca.* 1096 Ma main stage magmatic intervals within the Midcontinent Rift were voluminous and interpreted to be the result of a plume-related thermal anomaly. The interpretation that this volcanism is associated with a deep-seated mantle plume needs to be reconciled with the long duration of magmatism and rapid equatorward motion of Laurentia from a latitude of $\sim 54^\circ$ N *ca.* 1108 Ma during early stage flood basalt eruptions to $\sim 32^\circ$ N by *ca.* 1096 Ma (paleolatitudes for Duluth, MN). While some motion could be associated with true polar wander, in which the mesosphere and asthenosphere rotated in conjunction with the lithosphere, paleomagnetic pole positions require a substantial component of plate tectonic motion (Swanson-Hysell et al., 2019). The pulsed nature of magmatic activity could support an

164 interpretation of multiple upwelling pulses. As postulated by Cannon and Hinze (1992), the
165 initial pulse expressed by *ca.* 1108 early stage flood basalt volcanism initiated lithospheric
166 thinning. Given the significantly thinned lithosphere in the Midcontinent Rift region, subsequent
167 positively-buoyant plume material that encountered Laurentia lithosphere would have experienced
168 “upside-down” drainage wherein relief at the base of the lithosphere resulted in lateral and
169 upward flow into the Midcontinent Rift (Sleep, 1997; Swanson-Hysell et al., 2014). Flow of
170 upwelling mantle to locally-thin lithosphere would have led to ponding and concentrated
171 decompression melting within the rift. One scenario is that Laurentia was migrating over a plume
172 generation zone (Burke et al., 2008) from which multiple deep-seated mantle plumes upwelled and
173 reached the lithosphere during rift development. The first could have been centered on the
174 present-day Lake Superior region with the second encountering Laurentian lithosphere and being
175 directed to the rift by upside-down drainage in addition to driving magmatism in southwest
176 Laurentia. Another scenario is that *ca.* 1096 Ma magmatism was invigorated by upwelling return
177 flow enhanced by slab avalanche induced downwelling connected to the rapid plate motion of
178 Laurentia that initiated in the early stage (Swanson-Hysell et al., 2019). Overall, the constraint
179 that both the anorthositic and layered series of the Duluth Complex were emplaced in less than 1
180 million years requires an exceptional thermal anomaly that led to rapid and voluminous melt
181 generation during the main stage of Midcontinent Rift development.

182 ACKNOWLEDGEMENTS

183 Project research was supported by NSF EAR-1847277 (to NLS-H) and the University of
184 Minnesota Duluth. Funding for Boise State Isotope Geology Laboratory analytical infrastructure
185 was provided by NSF EAR-0824974 and EAR-0521221. Margaret Avery and Dan Costello
186 provided field assistance. Constructive reviews by Mauricio Ibañez-Mejia, Kyle Samperton, and
187 an anonymous referee improved the manuscript.

188 References

- 189 Beck, M., 1970, Paleomagnetism of Keweenawan intrusive rocks, Minnesota: *Journal of Geophysical Research*,
190 vol. 75, pp. 4985–4996, doi:10.1029/JB075i026p04985.
- 191 Blackburn, T. J., Olsen, P. E., Bowring, S. A., McLean, N. M., Kent, D. V., Puffer, J., McHone, G., Rasbury, E. T.,
192 and Et-Touhami, M., 2013, Zircon U-Pb geochronology links the end-Triassic extinction with the Central
193 Atlantic Magmatic Province: *Science*, vol. 340, pp. 941–945, doi:10.1126/science.1234204.
- 194 Bright, R. M., Amato, J. M., Denyszyn, S. W., and Ernst, R. E., 2014, U-Pb geochronology of 1.1 Ga diabase in the
195 southwestern United States: Testing models for the origin of a post-Grenville large igneous province:
196 *Lithosphere*, vol. 6, pp. 135–156, doi:10.1130/L335.1.
- 197 Burgess, S. D., Bowring, S. A., Fleming, T. H., and Elliot, D. H., 2015, High-precision geochronology links the
198 Ferrar large igneous province with early-Jurassic ocean anoxia and biotic crisis: *Earth and Planetary Science
199 Letters*, vol. 415, pp. 90–99, doi:10.1016/j.epsl.2015.01.037.
- 200 Burke, K., Steinberger, B., Torsvik, T. H., and Smethurst, M. A., 2008, Plume generation zones at the margins of
201 large low shear velocity provinces on the core–mantle boundary: *Earth and Planetary Science Letters*, vol. 265,
202 pp. 49–60, doi:10.1016/j.epsl.2007.09.042.
- 203 Cannon, W. F., 1992, The Midcontinent rift in the Lake Superior region with emphasis on its geodynamic
204 evolution: *Tectonophysics*, vol. 213, pp. 41–48, doi:10.1016/0040-1951(92)90250-A.
- 205 Cannon, W. F. and Hinze, W. J., 1992, Speculations on the origin of the North American Midcontinent rift:
206 *Tectonophysics*, vol. 213, pp. 49–55, doi:10.1016/0040-1951(92)90251-Z.
- 207 Condon, D. J., Schoene, B., McLean, N. M., Bowring, S. A., and Parrish, R. R., 2015, Metrology and traceability of
208 U–Pb isotope dilution geochronology (EARTHTIME tracer calibration part I): *Geochimica et Cosmochimica
209 Acta*, vol. 164, pp. 464–480, doi:10.1016/j.gca.2015.05.026.
- 210 Davis, D. and Green, J., 1997, Geochronology of the North American Midcontinent rift in western Lake Superior
211 and implications for its geodynamic evolution: *Canadian Journal of Earth Science*, vol. 34, pp. 476–488,
212 doi:10.1139/e17-039.
- 213 Edwards, G. H. and Blackburn, T., 2018, Detecting the extent of ca. 1.1 Ga Midcontinent Rift plume heating using
214 U-Pb thermochronology of the lower crust: *Geology*, vol. 46, pp. 911–914, doi:10.1130/g45150.1.
- 215 Fairchild, L. M., Swanson-Hysell, N. L., Ramezani, J., Sprain, C. J., and Bowring, S. A., 2017, The end of
216 Midcontinent Rift magmatism and the paleogeography of Laurentia: *Lithosphere*, vol. 9, pp. 117–133,
217 doi:10.1130/L580.1.
- 218 Green, J., 1983, Geologic and geochemical evidence for the nature and development of the Middle Proterozoic
219 (Keweenawan) Midcontinent Rift of North America: *Tectonophysics*, vol. 94, pp. 413–437,
220 doi:10.1016/0040-1951(83)90027-6.
- 221 Green, J. C., Boerboom, T. J., Schmidt, S. T., and Fitz, T. J., 2011, The North Shore Volcanic Group:
222 Mesoproterozoic plateau volcanic rocks of the Midcontinent Rift System in northeastern Minnesota: *GSA Field
223 Guides*, vol. 24, pp. 121–146, doi:10.1130/2011.0024(07).
- 224 Ibañez-Mejia, M. and Tissot, F. L. H., 2019, Extreme Zr stable isotope fractionation during magmatic fractional
225 crystallization: *Science Advances*, vol. 5, p. eaax8648, doi:10.1126/sciadv.aax8648.
- 226 Jaffey, A., Flynn, K., Glendenin, L., Bentley, W., and Essling, A., 1971, Precision measurement of half-lives and
227 specific activities of ^{235}U and ^{238}U : *Physical Review*, vol. C4, pp. 1889–1906, doi:10.1103/PhysRevC.4.1889.

- 228 Jirsa, M. A., Boerboom, T., Chandler, V., Mossler, J., Runkel, A., and Setterholm, D., 2011, S-21 Geologic map of
229 Minnesota-bedrock geology: Tech. rep., Minnesota Geological Survey, URL
230 <http://hdl.handle.net/11299/101466>.
- 231 Mattinson, J. M., 2005, Zircon U/Pb chemical abrasion (CA-TIMS) method: Combined annealing and multi-step
232 partial dissolution analysis for improved precision and accuracy of zircon ages: *Chemical Geology*, vol. 220, pp.
233 47–66, doi:10.1016/j.chemgeo.2005.03.011.
- 234 Miller, J., James D., Green, J. C., Severson, M. J., Chandler, V. W., and Peterson, D. M., 2001, M-119 Geologic
235 map of the Duluth Complex and related rocks, northeastern Minnesota: Tech. rep., Minnesota Geological Survey.
- 236 Miller, J., J.D., Green, J., Severson, M., Chandler, V., Hauck, S., Peterson, D., and Wahl, T., 2002, Geology and
237 mineral potential of the Duluth Complex and related rocks of northeastern Minnesota: Minnesota Geological
238 Survey Report of Investigations, vol. 58.
- 239 Nicholson, S. W. and Shirey, S. B., 1990, Midcontinent Rift Volcanism in the Lake Superior Region: Sr, Nd, and Pb
240 Isotopic Evidence for a Mantle Plume Origin: *J. Geophys. Res.*, vol. 95, pp. 10,851–10,868,
241 doi:10.1029/JB095iB07p10851.
- 242 Paces, J. and Miller, J., 1993, Precise U-Pb ages of Duluth Complex and related mafic intrusions, northeastern
243 Minnesota: Geochronological insights to physical, petrogenetic, paleomagnetic and tectonomagmatic processes
244 associated with the 1.1 Ga Midcontinent Rift System: *Journal of Geophysical Research*, vol. 98, pp.
245 13,997–14,013, doi:10.1029/93jb01159.
- 246 Schoene, B., Crowley, J. L., Condon, D. J., Schmitz, M. D., and Bowring, S. A., 2006, Reassessing the uranium
247 decay constants for geochronology using ID-TIMS U–Pb data: *Geochimica et Cosmochimica Acta*, vol. 70, pp.
248 426–445, doi:10.1016/j.gca.2005.09.007.
- 249 Schoene, B., Eddy, M. P., Samperton, K. M., Keller, C. B., Keller, G., Adatte, T., and Khadri, S. F. R., 2019, U-Pb
250 constraints on pulsed eruption of the Deccan Traps across the end-Cretaceous mass extinction: *Science*, vol. 363,
251 pp. 862–866, doi:10.1126/science.aau2422.
- 252 Sleep, N. H., 1997, Lateral flow and ponding of starting plume material: *Journal of Geophysical Research: Solid*
253 *Earth*, vol. 102, pp. 10,001–10,012, doi:10.1029/97JB00551.
- 254 Sprain, C. J., Renne, P. R., Vanderkluysen, L., Pande, K., Self, S., and Mittal, T., 2019, The eruptive tempo of
255 Deccan volcanism in relation to the Cretaceous-Paleogene boundary: *Science*, vol. 363, pp. 866–870,
256 doi:10.1126/science.aav1446.
- 257 Stein, C. A., Kley, J., Stein, S., Hindle, D., and Keller, G. R., 2015, North America’s Midcontinent Rift: When rift
258 met LIP: *Geosphere*, doi:10.1130/GES01183.1.
- 259 Swanson-Hysell, N. L., Ramezani, J., Fairchild, L. M., and Rose, I. R., 2019, Failed rifting and fast drifting:
260 Midcontinent Rift development, Laurentia’s rapid motion and the driver of Grenvillian orogenesis: *GSA Bulletin*,
261 doi:10.1130/b31944.1.
- 262 Swanson-Hysell, N. L., Vaughan, A. A., Mustain, M. R., and Asp, K. E., 2014, Confirmation of progressive plate
263 motion during the Midcontinent Rift’s early magmatic stage from the Osler Volcanic Group, Ontario, Canada:
264 *Geochemistry Geophysics Geosystems*, vol. 15, pp. 2039–2047, doi:10.1002/2013GC005180.
- 265 Tauxe, L., Shaar, R., Jonestrask, L., Swanson-Hysell, N., Minnett, R., Koppers, A., Constable, C., Jarboe, N.,
266 Gaastra, K., and Fairchild, L., 2016, PmagPy: Software package for paleomagnetic data analysis and a bridge to
267 the Magnetics Information Consortium (MagIC) Database: *Geochemistry, Geophysics, Geosystems*,
268 doi:10.1002/2016GC006307.
- 269 Vervoort, J., Wirth, K., Kennedy, B., Sandland, T., and Harpp, K., 2007, The magmatic evolution of the
270 Midcontinent rift: New geochronologic and geochemical evidence from felsic magmatism: *Precambrian Research*,
271 vol. 157, pp. 235–268, doi:10.1016/j.precamres.2007.02.019.

- 272 White, R. and McKenzie, D., 1995, Mantle plumes and flood basalts: Journal of Geophysical Research: Solid Earth
273 (1978–2012), vol. 100, pp. 17,543–17,585, doi:10.1029/95JB01585.